

# LZ PMT Thermal Neutron Activation Analysis

Junhui Liao, junhui\_liao@brown.edu,

Casey Rhyne, casey\_rhyne@brown.edu,

Department of Physics, Brown University, RI-02912, USA

Monday 19<sup>th</sup> June, 2017

## 1 Introduction

The LUX-ZEPLIN (LZ) experiment is a planned dual phase xenon time projection chamber constructed to search for dark matter in the form of weakly interacting massive particles (WIMPs). This dark matter detector will feature 494 Hammamatsu Model R11410-22 photo-multiplier tubes (PMTs) in the primary upper and lower PMT arrays as a detector for light signals generated within the detector as a result of particle interactions within the xenon. The LZ experiment aims to achieve world-leading sensitivity to a WIMP-nucleon spin-independent cross section of  $3 \times 10^{-48}$  cm<sup>2</sup>. To do so, backgrounds within the detector, including radioactivity stemming from activation of components of the detector, must be strictly controlled. Screening for activity in a variety of isotopes is conducted regularly to limit these backgrounds for all LZ detector components at the Sanford Underground Research Facility (SURF) in Lead, SD via on-site germanium detectors. Routine screening of PMTs at SURF has observed a significant increase in <sup>60</sup>Co above measured baseline levels for certain batches of screened PMTs.

The expected cause of this activation is thermal neutron capture on <sup>59</sup>Co within the PMT materials resulting from exposure to neutron sources present near the PMT storage and testing area at Brown University. Two potential nearby sources for thermal neutrons nearby have been identified at Brown: a stored <sup>252</sup>Cf source and a Deuterium-Deuterium (D-D) neutron generator. Activation will have occurred via the thermalization of fast neutrons given off by these sources during PMT storage on nearby materials, most significantly on hydrogenous material, followed by subsequent capture within the PMT. All PMTs that have been stored and tested at Brown during the period in which these neutron sources were present have been tracked to help build a reliable model for this neutron activation and to set limits on the maximum activation. This document attempts to explain the origin of all observed excess activation in <sup>60</sup>Co in the currently available PMT activation data from SURF, grouped into six PMT screening batches, and to establish an

exposure model to predict the activation of all PMTs that have passed through Brown during this neutron exposure period.

## 2 PMT Batching for Available Screening Results and Activation Sources

The location and potential exposure sources for the 6 batches of PMTs observed to have non-negligible activation in  $^{60}\text{Co}$  are shown in Figure 1. The groups are referred to as Batch 1 through Batch 6 based on the arrival date of the PMTs at Brown from earliest to latest. The three major sources of potential activation, the  $^{252}\text{Cf}$  source and the two D-D neutron generator testing runs in October and December, are considered individually to estimate the activation from each, and are notated in the top two rows of the chart.

The  $^{252}\text{Cf}$  source, which was stored in a shielded borated polyethylene castle in a cabinet in 040 (shown in Figure 2), provided a sustained low rate of thermal neutron flux at the nearby PMT storage locations, with a mean activity across the exposure period of  $(4.7 \pm 0.2) \times 10^6$  fast neutrons/second. The D-D generator (shown in Figure 3) was similarly housed inside a borated polyethylene castle, and was additionally surrounded by water shielding on three sides via two sets of water bricks and a filled water tank. While the D-D generator produced neutrons for significantly shorter periods of time than the  $^{252}\text{Cf}$  was present in the lab, it did so at a much higher intensity during these periods. Placement for the two sources is indicated in Figures 4 and 5, with distances relative to the relevant exposure locations provided in Table 6.

For batches 1,2, and 3, net  $^{60}\text{Co}$  activation levels were directly available via UK screening before arrival at Brown. Batch 4, like batches 1,2, and 3, was shipped from the UK, and so was assumed to have a  $1 \pm 1$  mBq baseline activity consistent with the other three. Batches 5 and 6 are expected to have negligible baselines.

To reconstruct the expected contributions of each neutron source to the overall activity in the PMTs tested at Brown, we examine the six batches in three sets of two batches each. Batches 5 and 6 arrived after all D-D runtime, and thus will be considered first as a cross-check against the expected  $^{252}\text{Cf}$ -based activation model constructed from  $^3\text{He}$  thermal neutron measurements with the  $^{252}\text{Cf}$  source present. Batches 3 and 4 will then be combined with the  $^{252}\text{Cf}$  activation model verified using batches 5 and 6 to estimate the activation resulting from the D-D generator run in December. Batches 1 and 2 will be similarly considered

### PMT Exposure History for Measured Activated Batches

\*Note: Overlaps indicate some PMTs from a batch were temporarily located in indicated secondary location.

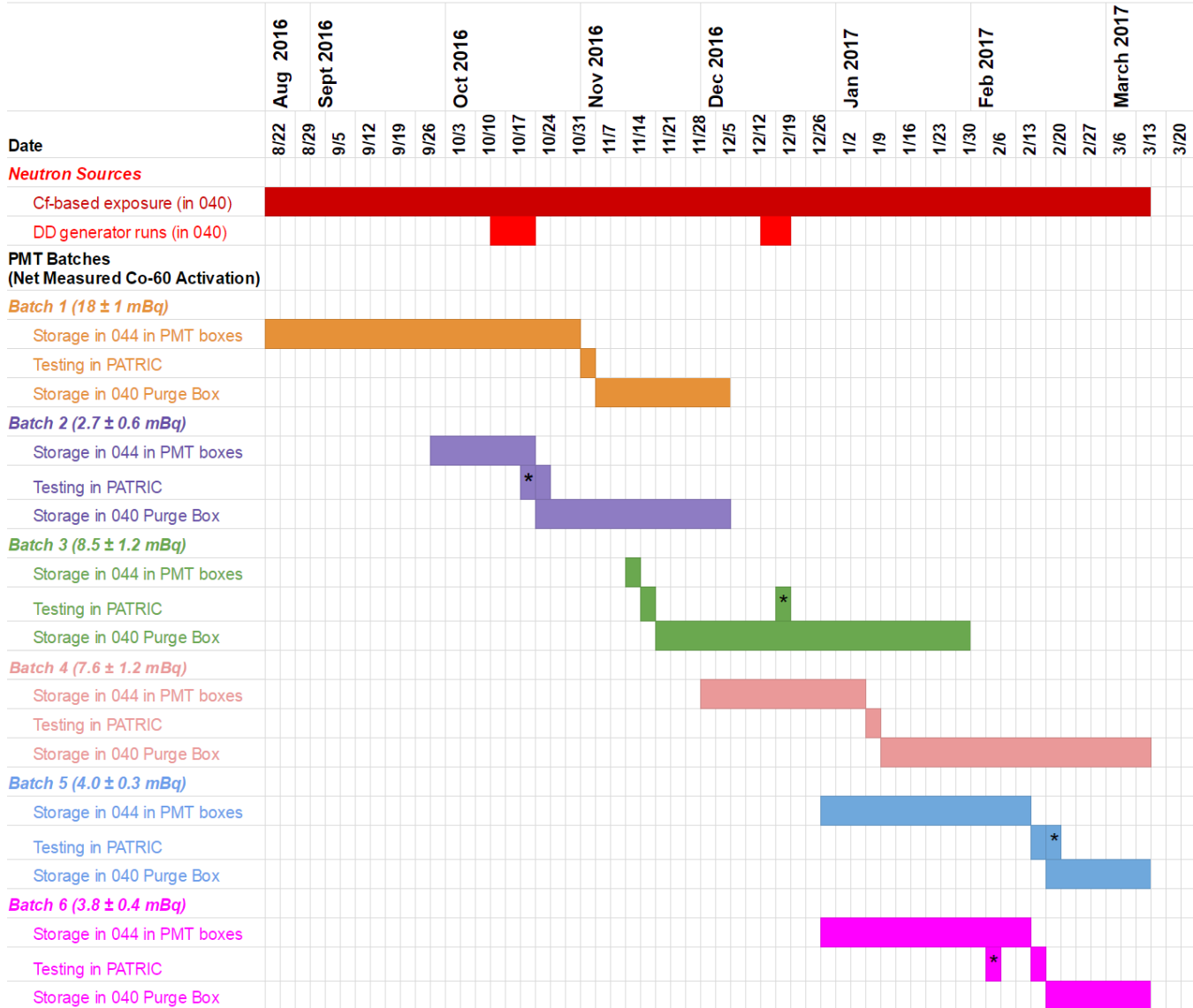


Figure 1: A timeline for placement and exposure for all 6 PMT batches with activity measured at SURF.

Exposure periods due to  $^{252}\text{Cf}$  and D-D neutron runs are labeled above the batches.



Figure 2: A picture of the borated polyethylene shielding for the  $^{252}\text{Cf}$  source. External shielding plates are 10 to 15 cm thick on front and top, 3 to 5 cm thick on the back, and surround a 30 cm diameter borated polyethylene tub housing the source.

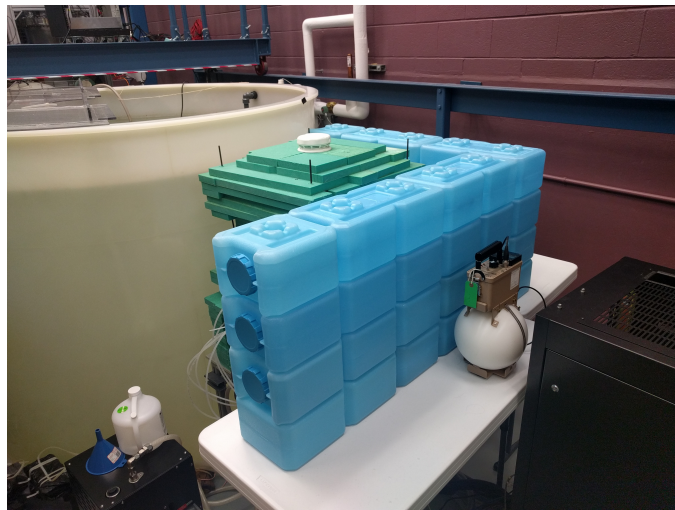


Figure 3: A picture of the Deuterium-Deuterium neutron generator, with shielding. A borated polyethylene castle of varying thickness (approximately 10 cm) surrounds the generator head. A 15 cm-thick wall of Water bricks on two sides and a filled 2 m diameter water tank on the third side further reduce the outwards flux of 2.45 MeV neutrons produced during runtime.

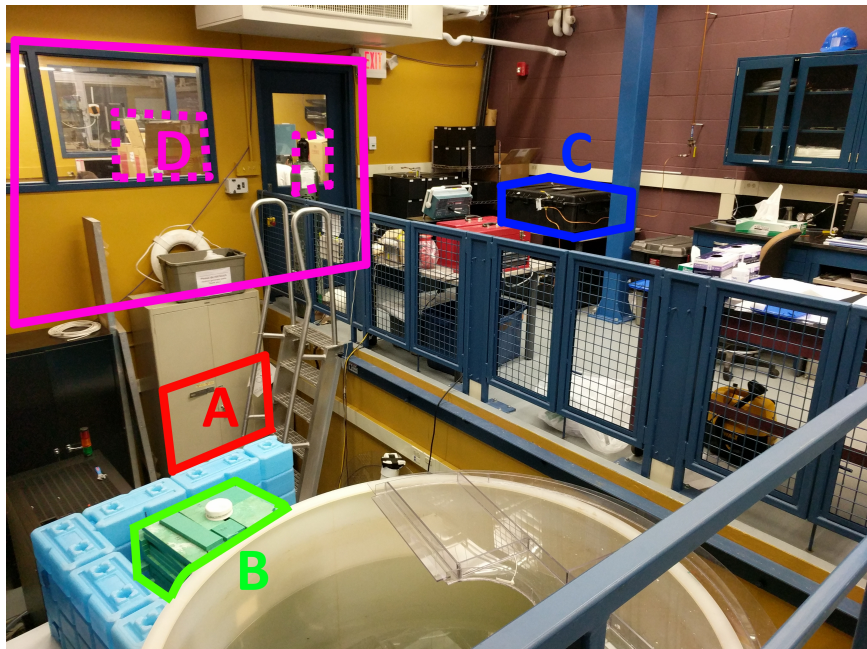


Figure 4: A photo taken within room 040 showing the locations of neutron sources within the lab and PMT exposure locations. ‘A’:  $^{252}\text{Cf}$  source location within borate polyethylene castle and storage cabinet. ‘B’: Neutron generator borated polyethylene shielding castle. The DD neutron source is centered within this castle, and is further surrounded by water shielding via a water tank and water bricks. ‘C’: Temporary PMT staging purge box to store PMTs before between final PATRIC testing and shipping out or storage in the Brown Clean Room. ‘D’: Room 044 Storage location for PMTs within original boxing before testing with PATRIC. Several common storage locations in 044 are outlined with dotted lines.

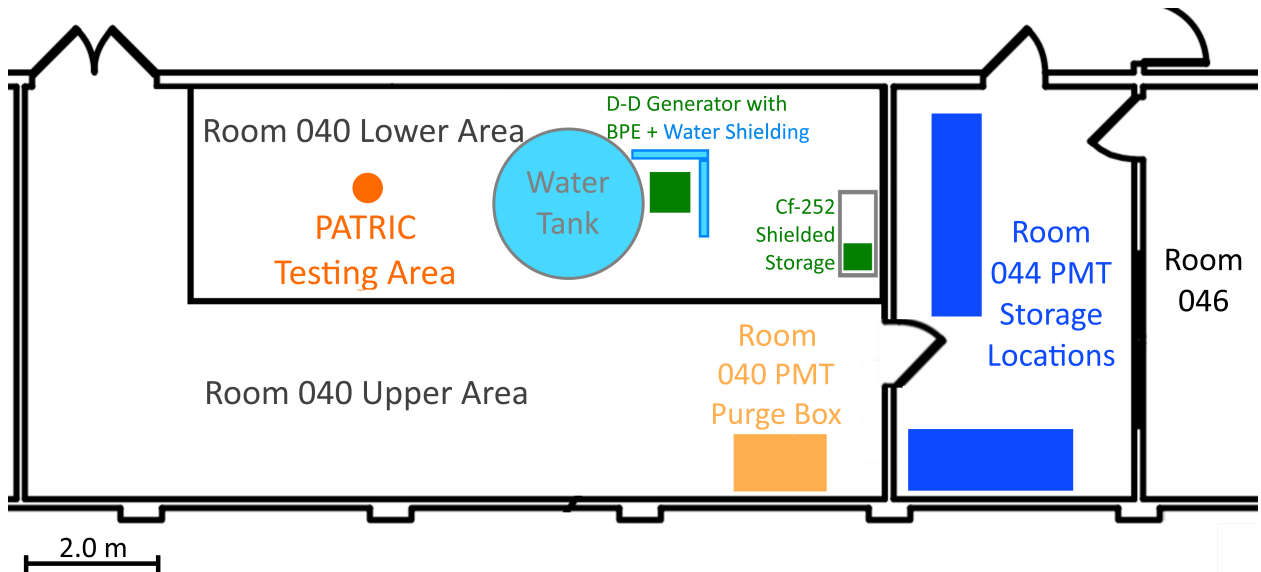


Figure 5: Plan view of the lab and relevant temporary PMT storage locations. Relevant distances are detailed in Table 6. DD generator and  $^{252}\text{Cf}$  locations indicate the footprint of the borated polyethylene neutron shielding, with each source centered within the structure.

to estimate the potential activation stemming from the October generator run. Lastly, the well-defined activation signal in batch 1 will be used to propose a cross-check between the expected activation model and the known generator output.

### 3 Validation of $^3\text{He}$ Sensitivity from Activation of PMT Batches 5 and 6

Batches 5 and 6 PMTs both arrived together at Brown on Dec 30, 2016, after the conclusion of all D-D generator activity. This provides a robust starting point for the comparison of expected and observed neutron activation contributed from the  $^{252}\text{Cf}$  source alone, since all observed net activation will have resulted from thermal neutron capture from this source alone. The two sets of PMTs were both present in the lab until the removal of the  $^{252}\text{Cf}$  source (March 17th), and both accumulated 78 days of exposure as a result. Batches 1 and 2 were measured to have identical activation within uncertainty ( $4.0 \pm 0.3$  and  $3.8 \pm 0.4$  mBq respectively), which was expected given their placement and timing throughout the lab during exposure was also nearly

identical (See Figure 1).

Estimates were made for the expected activation of batches 5 and 6 based on measurements of the thermal neutron flux taken with an LND 25185  $^3\text{He}$  proportional tube while the  $^{252}\text{Cf}$  source was stored in the lab. Repeated measurements upon the removal of the source at a later time showed a reduction in the thermal neutron rate by two orders of magnitude, so this background is treated as insignificant henceforth. Measurements using the  $^3\text{He}$  tube at each location in which PMTs were stored are listed in table 1, as well as the converted neutron flux and the estimated rate of activation per PMT for each location. The  $^3\text{He}$  tube sensitivity of  $0.60 \pm 0.06$  counts/(n/cm<sup>2</sup>) was provided by LND Inc [2], and was used to convert the measured counts rate to thermal neutron fluxes. This value is reasonable given the composition of the detector, and comparisons of this to expected values are discussed briefly in Section 8.1. The subsequent conversion factor from thermal neutron flux to mBqs of  $^{60}\text{Co}$  is  $(8.1 \pm 0.7) \times 10^{-3}$  ( $\mu\text{Bq}/\text{PMT}$ )/(n/cm<sup>2</sup>), and is calculated in Section 8.2.

Table 1: Thermal neutron measurements and expected rate of  $^{252}\text{Cf}$ -based Activation

Location	$^3\text{He}$ rate (cpm)	Measured thermal neutron flux (n/cm <sup>2</sup> /min)	Activation/day ( $\mu\text{Bq}/\text{PMT}/\text{day}$ )
044 Storage (Various)	$2.5 \pm 1.3$ <sup>a</sup>	$4.2 \pm 2.2$	$48 \pm 26$
040 Purge Box	$3.6 \pm 0.3$	$6.0 \pm 0.8$	$70 \pm 11$
In PATRIC	$1.0 \pm 0.3$	$1.7 \pm 0.5$	$19 \pm 6$

<sup>a</sup> The quoted  $^3\text{He}$  count rate in 044 is a summary of several locations within the room with spreads from  $1.8 \pm 0.6$  to  $3.0 \pm 0.8$  cpm. PMT Position within this room was not documented, so the uncertainty in the rate of activation for each PMT is higher than usual.

Combining the activation rates listed in Figure 1 with the recorded placement and duration of exposure for batches 5 and 6 yields an expected activation of  $4.0 \pm 1.2$  and  $4.2 \pm 1.1$  mBq/PMT, which is consistent with the observed activities ( $4.0 \pm 0.3$  and  $3.8 \pm 0.4$  mBq/PMT). This agreement allows us to use these measurements to confidently estimate the  $^{252}\text{Cf}$ -based exposure for the remaining batches.

Table 2:  $^{252}\text{Cf}$ -based exposure summary for Batches 5 and 6

Batch	Time in	Time in	Total Expected	SURF-Measured
	044	040	$^{252}\text{Cf}$ Activation	Net Activation
	(days)	(days)	(mBq)	(mBq)
5	45	26	$4.0 \pm 1.2$	$4.0 \pm 0.3$
6	26	31	$4.2 \pm 1.1$	$3.8 \pm 0.4$

## 4 Estimation of DD-based Activation from Batches 3 and 4

The two measured PMT batches arriving in November and December of 2016 (batches 3 and 4) can be used to estimate the neutron activation from the D-D generator. Both PMT batches were present in the lab during only the second generator run (December 16th - 22nd) and have been measured to have consistent activation in  $^{60}\text{Co}$  ( $8.5 \pm 1.2$  and  $7.6 \pm 1.2$  mBq/PMT respectively). Combining the  $^{252}\text{Cf}$  activation rates established in the previous section with the PMT placement for batches 3 and 4 detailed in Section 2, we estimate in Table 3 the rate of  $^{252}\text{Cf}$ -based activation in each batch and compare to each one's observed activation.

Table 3:  $^{252}\text{Cf}$ -based exposure summary for Batches 3 and 4

Batch	Time in	Time in	Total Expected	SURF-Measured	Implied D-D-based
	044	040	$^{252}\text{Cf}$ Activation	Net Activation	Activation
	(days)	(days)	(mBq)	(mBq)	(mBq)
3	2	71	$5.0 \pm 0.7$	$8.5 \pm 1.2$	$3.5 \pm 1.4$
4	33	68	$6.3 \pm 1.1$	$7.6 \pm 1.2$	$1.3 \pm 1.7$

From the difference in predicted  $^{252}\text{Cf}$  and total observed activation, this suggests the D-D generator's contribution to  $^{60}\text{Co}$  activation to be  $3.5 \pm 1.4$  mBq/PMT in batch 3 and  $1.3 \pm 1.7$  mBq/PMT in batch 4, with expected variations in position-dependent thermal neutron rates accounting for the difference in activation to each [1].

## 5 PMT Placement and Activation in Batches 1 and 2

Batches 1 and 2 are recorded to have similar exposure profiles, with both being recorded spending several months at Brown throughout October and November and observing only the first D-D neutron generator run from the same general location (Room 044). Despite this similarity, the overall activation in  $^{60}\text{Co}$  has been measured to be significantly higher in batch 1 than batch 2. Similarly to the earlier batches, we can apply the  $^3\text{He}$ -based projections from Section 3 to estimate the contribution due to  $^{252}\text{Cf}$  and infer activation due to the October D-D run observed by both. From batch 1, we expect  $5.4 \pm 1.8$  of the  $18.1 \pm 1.1$  mBq of activation per PMT from  $^{252}\text{Cf}$ , which implies  $12.7 \pm 2.1$  mBq/PMT from D-D. From batch 2, we expect  $4.1 \pm 0.8$  mBq/PMT of activation from  $^{252}\text{Cf}$  alone and observe a net activation  $2.7 \pm 0.6$ , which implies no significant activation from the October D-D generator run.

Table 4:  $^{252}\text{Cf}$ -based exposure summary for Batches 1 and 2

Batch	Time in 044 (days)	Time in 040 (days)	Total Expected $^{252}\text{Cf}$ Activation (mBq)	SURF-Measured Net Activation (mBq)	Implied D-D-based Activation (mBq)
1	68	31	$5.4 \pm 1.8$	$18.1 \pm 1.0$	$12.7 \pm 2.1$
2	25	41	$4.1 \pm 0.8$	$2.7 \pm 0.6$	- <sup>a</sup>

<sup>a</sup> Results imply that Batch 2 was not exposed to D-D neutrons, and was stored in 046 during generator runtime.

Despite the regular and systematic documentation of PMT shipment arrival times and departures and movement into and out of the PATRIC testing area, the exact location of each box of PMTs before unpacking and testing is not recorded. While ordinarily, most PMTs are stored in varying locations in the 044 storage area, some PMT boxes were occasionally stored in room 046, a room significantly further from both the  $^{252}\text{Cf}$  and D-D sources, which results in roughly one order smaller thermal neutron exposure. Given the significantly lower activation observed, it is likely that this batch was placed in this location rather than 044 before being tested in PATRIC. Results from further screening at SURF of PMTs that followed batches 1 and 2 are pending, and could help confirm this placement.

## 6 Potential Model Test via D-D $^3\text{He}$ Measurement

We can use the low relative uncertainty in the expected D-D activation from  $^{252}\text{Cf}$  subtraction from batch 1 as a means of testing our model for thermal neutron activation. Using the established  $^3\text{He}$  sensitivity  $S$  and the PMT conversion factor  $C_{mBq,PMT}$  discussed in Sections 8.1 and 8.2, we can convert backwards from  $A_{obs}$ , the projected  $12.7 \pm 2.1$  mBq of activation from the October D-D run to an expected total number of counts observable in the  $^3\text{He}$  tube via:

$$\begin{aligned} N_{counts,exp} &= A_{obs}/C_{mBq,PMT} \times S \\ &= [12.7 \pm 2.1 \text{ mBq/PMT}]/[8.1 \pm 0.7 \times 10^{-3}(\mu\text{Bq/PMT})/(\text{neutron/cm}^2)] \times [0.60 \pm 0.06 \text{ counts}/(\text{neutron/cm}^2)] \\ &= (9.4 \pm 2.0) \times 10^5 \text{ counts} \end{aligned}$$

Since the fast neutron intensity and duration of runtime for the October D-D generator run were well documented (via periodic Bonner sphere measurements), we can divide  $N_{counts,exp}$  by the total generator runtime (160 hours) to estimate the expected measurable  $^3\text{He}$  count rate  $R_{exp}$  for the generator set to the mean run flux of  $(4.2 \pm 0.7) \times 10^7$  n/s as

$$\begin{aligned} R_{exp} &= (9.4 \pm 2.0) \times 10^5 \text{ counts}/(160 \text{ hours}) \\ &= 100 \pm 20 \text{ cpm expected} \end{aligned}$$

for measurements taken at the 040 PMT purge box, where PMTs were stored at the time of the D-D run.

## 7 Conclusions

Combining location-based thermal neutron flux measurements with observed activities and known PMT placement, we establish a model for PMT activation that sets a limit on the overall activation from exposure to both neutron sources housed at Brown. Activation due to long-term exposure to the  $^{252}\text{Cf}$  source are consistent with expectations, and are limited to below 7 mBq for all PMTs tested at Brown. Activation due to the D-D generator tests is mostly confined to the first of the two runs, and activation from this run is limited to 13 mBq. All 20 additional unscreened PMTs exposed to this run are queued to be evaluated for activation at SURF. Upcoming results from SURF screening of queued PMT batches and the allowance of  $^3\text{He}$  measurements of D-D-based thermal neutron fluxes at the locations of PMT exposure could help reduce

uncertainties in the model arising from imperfect PMT location tracking.

Table 5: Summary of  $^{60}\text{Co}$  Activation per Batch

Batch	SURF-measured Activation (mBq)	$^{252}\text{Cf}$ Activation (mBq)	D-D Activation (mBq)
1	$18.1 \pm 1.0$	$5.4 \pm 1.8$	$12.7 \pm 2.8$
2	$2.7 \pm 0.6$	$4.1 \pm 0.8$	- <sup>a</sup>
3	$8.5 \pm 1.2$	$5.0 \pm 0.7$	$3.5 \pm 1.4$
4	$7.6 \pm 1.2$	$6.3 \pm 1.1$	$1.3 \pm 1.7$
5	$4.0 \pm 0.3$	$4.0 \pm 1.2$	0
6	$3.8 \pm 0.4$	$4.2 \pm 1.1$	0

<sup>a</sup> Results imply that Batch 2 was not exposed to D-D neutrons, and was stored in 046 during generator runtime.

## 8 Appendix

### 8.1 Appendix A: Sensitivity of the $^3\text{He}$ Tube

To measure thermal neutron fluxes at exposure points throughout the lab, an LND 25185  $^3\text{He}$  Tube was used. Specifications provided by the company state that the given sensitivity of this tube to thermal neutrons is  $0.60 \pm 0.06$  counts/(neutron/cm<sup>2</sup>). As a cross-check against this provided sensitivity, we estimate the ideal sensitivity of the tube given the physical parameters of the  $^3\text{He}$  target. From the manufacturer-provided effective volume and gas pressure at room temperature, we find the number of  $^3\text{He}$  atoms  $N$  in the target to be

$$\begin{aligned} N &= (2.00 \pm 0.01 \text{ atm}) \times (4.5 \pm 0.1 \text{ cm}^3) / (1.36 \times 10^{-22} \text{ cm}^3 \cdot \text{atm} \cdot \text{K}^{-1}) / (298 \text{ K}) \\ &= (2.22 \pm 0.06) \times 10^{20} \text{ }^{59}\text{Co atoms/PMT} \end{aligned}$$

From the definition of sensitivity  $S$ , we divide the total number of interactions expected for a target with no self-shielding,  $N\sigma\phi$ , where  $\sigma$  is the cross section for thermal neutron capture of  $^3\text{He}$ , or  $(5.3 \pm 0.1) \times 10^{-21} \text{ cm}^2$  [5],

by a known flux  $\phi$ . Thus,

$$\begin{aligned} S &= N\sigma \\ &= (2.22 \pm 0.06) \times 10^{20} \times (5.3 \pm 0.1) \times 10^{-21} \text{ cm}^2 \\ &= 1.18 \pm 0.04 \text{ counts}/(\text{neutron/cm}^2) \end{aligned}$$

Comparing the ideal and quoted sensitivities, this suggests a detection efficiency of  $0.60/1.18 = 51\%$  for incident thermals stemming from the relatively low-pressure of the  ${}^3\text{He}$  gas.

## 8.2 Appendix B: Conversion Factor for PMT Activation via $^{59}\text{Co} + n \rightarrow ^{60}\text{Co} + \gamma$

To calculate the expected activation per PMT by thermal neutrons, we establish a conversion factor  $C_{N,PMT}$  to convert from a thermal neutron fluence to an expected thermal neutron capture rate within each PMT. The only components within each PMT with any appreciable  ${}^{59}\text{Co}$  are two Kovar flanges, each with a thickness of approximately 0.6 mm. As each flange is significantly thinner than the thermal neutron mean free path through the material, there is no self-shielding effect to consider (as in the  ${}^3\text{He}$  tube), and the expected activation efficiency reduces to a product of the scattering cross-section and the total number of  ${}^{59}\text{Co}$  atoms per PMT. Summing up the total mass of the two flanges (18 and 14 g) and multiplying by the percent composition of  ${}^{59}\text{Co}$  by weight of  $16 \pm 1\%$  [4] gives a total  ${}^{59}\text{Co}$  mass of

$$m_{{}^{59}\text{Co}} = (18 + 14 \text{ g}) \times (16 \pm 1\%) = (5.1 \pm 0.3) \text{ g } {}^{60}\text{Co/PMT}$$

After converting to the number of target atoms per PMT via  $A_r$ , the relative atomic mass of  ${}^{59}\text{Co}$ , and  $N_A$ , Avogadro's number, we multiply this by the cross-section for radiative neutron capture  $\sigma$  at the mode energy for thermal neutrons ( $37 \pm 2$  b [5] at the 0.025 eV peak) to obtain  $C_{N,PMT}$ , the overall thermal conversion factor per PMT:

$$\begin{aligned} C_{N,PMT} &= N_{{}^{59}\text{Co}} \sigma \\ &= (m_{{}^{59}\text{Co}}/A_r \times N_A) \times \sigma \\ &= (5.1 \pm 0.3 \text{ g})/(58.9 \text{ g/mol}) \times 6.02 \times 10^{23} \text{ mol}^{-1} \times ((37 \pm 2) \times 10^{-24} \text{ cm}^2) \\ &= 1.94 \pm 0.16 \text{ (} {}^{60}\text{Co atoms/PMT})/(\text{neutron/cm}^2) \end{aligned}$$

Dividing this result by the  ${}^{60}\text{Co}$  mean lifetime of 7.6 years provides a conversion factor for the expected activation per PMT per thermal neutron flux of  $C_{mBq,PMT} = (8.1 \pm 0.7) \times 10^{-3} (\mu\text{Bq/PMT})/(\text{neutron/cm}^2)$ .

### 8.3 Appendix C: Thermal Neutron Conversion Efficiency of the $^{252}\text{Cf}$ source

When the  $^{252}\text{Cf}$  source is present in Room 040 and the D-D generator is off, the only source of thermal neutrons should come from the Cf, as the environmental thermal neutrons are ignorable according to our analysis in the previous section. In principle, we should be able to observe the intensity of thermal neutrons changing inversely proportionally to the distances between the source and places of measurement. The measured locations can be seen in Figure 5.

The thermal neutron intensity of the source  $I$  can be estimated for each point of measurement via the measured thermal neutron flux  $\phi$  and the distance from the source  $R$  as:

$$I = \phi \times (4\pi R^2)$$

It is shown through agreement of the relative intensities that the estimated thermal neutron production profile is consistent with a  $1/r^2$  law. It is expected that the estimated flux of the P3 (PATRIC table) position deviates slightly below the values measured at other positions due to the presence of a water tank between the  $^{252}\text{Cf}$  source and the PATRIC table, which absorbs some thermal neutrons. The  $^{252}\text{Cf}$  source at the time of measurement had a known flux of fast neutrons (spectrum peaking at 1 MeV [3]) of  $(4.2 \pm 0.2) \times 10^6$  n/s, which implies  $(5 \pm 1)\%$  of the fast neutrons emitted have been moderated to be thermal ones in the lab.

Table 6: Measured and estimated thermal neutrons of the  $^{252}\text{Cf}$  source

Measuring position	Distance to $^{252}\text{Cf}$	Measured counts	Measured flux	Estimated $^{252}\text{Cf}$ Int.
	(cm)	(cpm)	(n/cm <sup>2</sup> /min)	(n/min)
P1 (PMT purge box in 040)	405 cm	$3.57 \pm 0.34$	$6.0 \pm 0.8$	$(12.3 \pm 1.7) \times 10^6$
P2 (“Bridge”)	626 cm	$1.60 \pm 0.33$	$2.7 \pm 0.6$	$(13.1 \pm 3.0) \times 10^6$
P3 (PATRIC table)	730 cm	$0.94 \pm 0.26$	$1.6 \pm 0.8$	$(10.5 \pm 3.1) \times 10^6$
P4 (Far corner of room 040)	1123 cm	$0.47 \pm 0.12$	$0.8 \pm 0.2$	$(12.4 \pm 3.4) \times 10^6$

An analogous evaluation could be performed with the D-D generator as well to compare the efficiency of conversion between the two energy spectra and shielding setups and over multiple locations.

## References

- [1] While both PMT batches were present for the entirety of the December D-D run, their placement is expected to influence the degree of activation in each. Batch 3 PMTs were primarily stored in the 040 purge box, while those in batch 4 was stored in 040 PMT storage. Given that the relative distance to the D-D generator is up to  $1.5\times$  greater than to the PMT purge box, we can expect to see up to a  $2\times$  reduction in activation from the D-D between locations.
- [2] Sensitivity and physical parameters of  $^3\text{He}$  tube obtainable at <http://lndinc.com/products/536/>. Uncertainty on sensitivity obtained from direct correspondence with LND, Inc.
- [3] Smith, A., Fields, P. and Roberts, J. (1957). Spontaneous Fission Neutron Spectrum of Cf252. Physical Review, 108(2), pp.411-413.
- [4] Information on PMT composition obtained from confidential correspondence with Hammamatsu
- [5] Cross-sectional scattering information used the JENDL-4.0 Database